Eur. Phys. J. D **28**, 171–179 (2004)
DOI: 10.1140/epjd/e2003-00308-1

THE EUROPEAN PHYSICAL JOURNAL D

Circular Rydberg states of hydrogenlike systems in collinear electric and magnetic fields of arbitrary strengths: an exact analytical classical solution

E. Oks[a]

Physics Department, Auburn University, Auburn, AL 36849-5311, USA

Received 24 February 2003 / Received in final form 6 June 2003
Published online 9 December 2003 –

Abstract. We derived analytical expressions for the energy of classical Circular Rydberg States (CRS) in collinear electric (**F**) and magnetic (**B**) fields of arbitrary strengths. Previously published explicit expressions for the energy E were given only for the region of a weak electric field F and only in the limits of $B \to 0$ and $B \to \infty$. We offered formulas for the dependence of the classical ionization threshold $F_c(B)$ and of the energy at this threshold $E_c(B)$ valid for the magnetic field B of an arbitrary strength. We also analyzed the stability of the motion by going beyond the CRS. In addition, for two important particular cases previously studied in the literature — classical CRS in a magnetic field only and classical CRS in an electric field only — we presented some new results as well.

PACS. 32.60.+i Zeeman and Stark effects – 31.15.-p Calculations and mathematical techniques in atomic and molecular physics (excluding electron correlation calculations)

1 Introduction

Circular Rydberg States (CRS) of hydrogenlike systems correspond to $|m| = n - 1 \gg 1$, where m and n are magnetic and principal quantum numbers, respectively. CRS have been extensively studied both theoretically and experimentally for several reasons (see, e.g., [1–4] and references therein). First, CRS have long radiative lifetimes and highly anisotropic collision cross-sections, thus enabling experimental works on inhibited spontaneous emission, cold Rydberg gases etc. [5–7]. Second, classical CRS correspond to quantal coherent states that are objects of fundamental importance. Third, a classical description of CRS serves as the primary term in the quantal method based on the $1/n$-expansion (see, e.g. [8] and references therein).

In the present paper we focus at analytical classical description of CRS in collinear electric (**F**) and magnetic (**B**) fields. This subject was previously studied in [8]. However, in paper [8], explicit expressions for the energy E were given only for the region of a weak electric field F and only in the limits of $B \to 0$ and $B \to \infty$. Below we present expressions for the energy E for arbitrary strengths of the electric and magnetic fields. Besides, the authors of [8] presented a dependence of the classical ionization threshold $F_c(B)$ only for the limits $B \to 0$ and $B \to \infty$ and they did not present at all the dependence of the energy at the ionization threshold $E_c(B)$. Below we offer formulas for $F_c(B)$ and $E_c(B)$ covering the entire range of B.

We note that two important particular cases were also previously studied analytically: classical CRS in a magnetic field only [9] and classical CRS in an electric field only [9,10][1].

In [9], the dependence of the energy E on the magnetic field B was presented, in fact, in a one-parametric form: $\{E(u),\ B(u)\}$. However, this problem allows a direct (non-parametric) analytical solution $E(B)$ that we present below. In [9,10], the study of classical CRS in an electric field was almost complete. Below we complement it only with a universal plot of a scaled energy versus a scaled electric field, thus presenting all possible subcases for this problem in one curve.

We structure our presentation as follows. In Section 2 we introduce scaled variables and the scaled Hamiltonian for classical CRS in collinear electric and magnetic fields. In Section 3 we present analytical results for classical CRS in a magnetic field only. In Section 4 we present analytical results for classical CRS in an electric field only. Sections 3 and 4 contain some new results and also serve as benchmarks facilitating a better physical understanding

[a] e-mail: goks@physics.auburn.edu

[1] List of various kinds of numerous works on a hydrogen atom in a magnetic field (not limited by the analytical classical description of CRS) can be found, e.g., in books [11,12]. The book [12] covers also various kinds of works on a hydrogen atom in an electric field (not limited by the analytical classical description of CRS).

of the general case: analytical classical description of CRS in collinear electric and magnetic fields. The latter is presented in Section 5. In Section 6 we summarize new results of this study.

2 Scaled variables and the scaled Hamiltonian

We consider a hydrogenlike system (atom or ion), where the nucleus of the charge Z is stationary at the origin. The system is subjected to collinear electric ($\mathbf{F}$) and magnetic ($\mathbf{B}$) fields. We choose the Oz-axis along the direction of the electric field $\mathbf{F}$ ($F_z > 0$). The magnetic field can be parallel to $\mathbf{F}$ ($B_z > 0$), or antiparallel to $\mathbf{F}$ ($B_z < 0$), or equal to zero. We confine ourselves with circular orbits of the electron (except Appendix, where this assumption is relaxed): the orbit, whose plane is perpendicular to Oz, has a radius ρ and its center is at the Oz-axis at some point z. In the cylindrical coordinates, by using the atomic units $e = m_e = 1$, the classical Hamilton function (hereafter, for brevity — Hamiltonian) can be written in the form:

$$H(\rho, z) = M^2/(2\rho^2) - Z/(\rho^2+z^2)^{1/2} + Fz + \Omega M + \Omega^2\rho^2/2,$$
$$\Omega \equiv B/(2c). \quad (1)$$

Here M = const. is the z-component of the angular momentum, Ω is the Larmor frequency. A practical formula for the Larmor frequency reads: $\Omega(\mathrm{s}^{-1}) \approx 8.794 \times 10^6 B(\mathrm{G})$.

We introduce the following scaled quantities:

$$u \equiv \rho Z/M^2, \quad w \equiv zZ/M^2, \quad f \equiv FM^4/Z^3,$$
$$\omega \equiv \Omega M^3/Z^2, \quad \varepsilon \equiv EM^2/Z^2, \quad (2)$$

where E is the energy. In the scaled variables, we get the following expression for the scaled Hamiltonian $h \equiv HM^2/Z^2$:

$$h(u, w) = 1/(2u^2) - 1/(u^2+w^2)^{1/2} + fw + \omega + \omega^2u^2/2. \quad (3)$$

Below we study, first of all, two important particular cases where either the electric field is zero or the magnetic field is zero. Then we analyze the general case represented by the scaled Hamiltonian from equation (3).

3 Classical circular Rydberg states in a magnetic field of an arbitrary strength

In this purely "magnetic" case, the scaled Hamiltonian simplifies as follows:

$$h_m(u, w) = 1/(2u^2) - 1/(u^2+w^2)^{1/2} + \omega + \omega^2u^2/2. \quad (4)$$

The conditions of the dynamic equilibrium are:

$$\partial h_m/\partial u = -1/u^3 + u/(u^2+w^2)^{3/2} + \omega^2 u = 0, \quad (5)$$
$$\partial h_m/\partial w = w/(u^2+w^2)^{3/2} = 0. \quad (6)$$

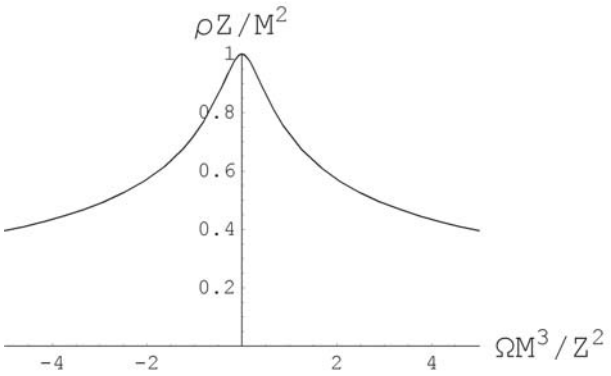

Fig. 1. Dependence of the scaled radius of the orbit $\rho Z/M^2$ on the scaled magnetic field $\Omega M^3/Z^2$ at the absence of the electric field (Ω is the Larmor frequency).

Therefore, $w = 0$ and from equation (5) we get:

$$\omega^2u^4 + u - 1 = 0. \quad (7)$$

By changing the variable

$$s \equiv u|\omega|^{2/3}, \quad (8)$$

we transform equation (7) into:

$$s^4 + s - |\omega|^{2/3} = 0. \quad (9)$$

By solving equation (9) analytically and using the relation (8), we obtain the following equilibrium value of u:

$$u = g(|\omega|^{2/3})/|\omega|^{2/3}, \quad (10)$$

where

$$g(x) \equiv \left\{2/[j(x)]^{1/2} - j(x)\right\}^{1/2}/2 - [j(x)]^{1/2}/2, \quad (11)$$

$$j(x) \equiv \left\{1/2 + \left[3\left(27 + 256x^3\right)\right]^{1/2}/18\right\}^{1/3} - (4x/3)/\left\{1/2 + \left[3\left(27 + 256x^3\right)\right]^{1/2}/18\right\}^{1/3}. \quad (12)$$

Figure 1 shows the dependence $u(\omega)$. It is seen that the larger the magnetic field, the more it compresses the orbit.

Substituting $w = 0$ and u from equation (10) into equation (4), we obtain the following result for the dependence of the scaled energy ε_m on the scaled magnetic field ω:

$$\varepsilon_m = |\omega|^{4/3}/\left\{2\left[g\left(|\omega|^{2/3}\right)\right]^2\right\} - |\omega|^{2/3}/g\left(|\omega|^{2/3}\right) + \omega + |\omega|^{2/3}\left[g\left(|\omega|^{2/3}\right)\right]^2/2. \quad (13)$$

We note that in [9] the corresponding result was not obtained in the direct form, like equation (13), but only in an indirect, parametric form.

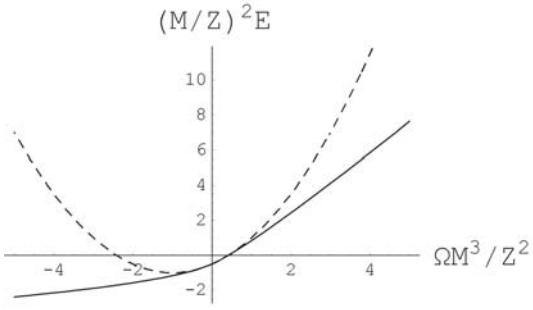

Fig. 2. Dependence of the scaled energy EM^2/Z^2 on the scaled magnetic field $\Omega M^3/Z^2$ at the absence of the electric field: the solid line shows our result; the dashed line represents the corresponding quantal result by Braun [12] valid only for relatively small magnetic fields.

It is instructive to compare our classical result for ε_m with the corresponding quantal result by Braun [13]. For CRS, i.e. $|m| = n - 1$, his result is as follows:

$$\varepsilon_{m,B} \approx -1/2 + \omega + \omega^2/2 \pm (2N_\pm + 1)\omega^2/n;$$
$$N_\pm = 0, 1, 2, \ldots; \quad N_\pm \ll n. \quad (14)$$

On the one hand, the quantal result includes a "fine structure", which is absent in our classical result (13): it is the last term in equation (14), which is much smaller than the previous term since $N_\pm \ll n$. On the other hand, the quantal result is valid only for small values of the scaled magnetic field $|\omega| \ll 1$, while our classical result is valid for arbitrary values of the magnetic field, including the strong field region. The quantal small-field result by Braun [13] corresponds only to the first three terms of the Taylor expansion of ε_m from equation (13) and does not reproduce higher order terms.

Figure 2 shows the dependence $\varepsilon_m(\omega)$ by a solid line. The difference in the shape of this curve between the regions $\omega > 0$ and $\omega < 0$ is due to the third (paramagnetic) term in equation (13). Physically, the region $\omega > 0$ corresponds to a positive projection of the angular momentum $\mathbf{M}$ on the magnetic field $\mathbf{B}$, while the region $\omega < 0$ corresponds to a negative projection of $\mathbf{M}$ on $\mathbf{B}$. The dashed curve in Figure 2 represents the corresponding quantal result by Braun [13] (without the small "fine structure" term). It is seen that the quantal result becomes less and less accurate with the increase of $|\omega|$.

The plots in Figures 1 and 2 are universal: due to the employment of the scaled quantities, they present the results for the radius of the orbit ρ at the equilibrium and for the energy E for all possible sets of M, Z, and B.

4 Classical circular Rydberg states in an electric field of an arbitrary strength

In this purely "electric" case, the scaled Hamiltonian from equation (3) simplifies as follows:

$$h_e(u, w) = 1/\left(2u^2\right) - 1/\left(u^2 + w^2\right)^{1/2} + fw. \quad (15)$$

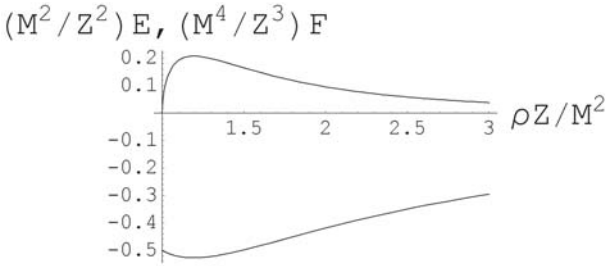

Fig. 3. Dependence of the scaled energy EM^2/Z^2 (the lower curve) and of the scaled electric field FM^4/Z^3 (the upper curve) on the scaled radius of the orbit $\rho Z/M^2$ at the absence of the magnetic field.

The conditions of the dynamic equilibrium are:

$$\partial h_e/\partial u = -1/u^3 + u/\left(u^2 + w^2\right)^{3/2} = 0, \quad (16)$$

$$\partial h_e/\partial w = w/\left(u^2 + w^2\right)^{3/2} + f = 0. \quad (17)$$

From equation (16) we find the following relation between the equilibrium values of w and u:

$$w(u) = -u\left(u^{2/3} - 1\right)^{1/2}. \quad (18)$$

Using equations (17, 18), we express the scaled electric field f via the scaled radius of the orbit u:

$$f(u) = \left(u^{2/3} - 1\right)^{1/2}/u^3. \quad (19)$$

Substituting $w(u)$ and $f(u)$ from equations (18, 19) into equation (15), we obtain the following result for the dependence of the scaled energy ε_e on the scaled radius of the orbit u:

$$\varepsilon_e(u) = 3/(2u^2) - 2/u^{4/3}. \quad (20)$$

Equations (19, 20) represent the dependence of the scaled energy ε_e on the scaled electric field f in the one-parametric form $\{\varepsilon_e(u), f(u)\}$.

Figure 3 shows the dependencies $\varepsilon_e(u)$ and $f(u)$ — the lower and upper curves, respectively. It is seen that both $\varepsilon_e(u)$ and $f(u)$ have an extremum. From equations $d\varepsilon_e/du = 0$ and $df/du = 0$ it is easy to find, that both $\varepsilon_e(u)$ and $f(u)$ reach their extrema at the same point $u_0 = (9/8)^{3/2} \approx 1.19324$, the values of the extrema being: $\varepsilon_e(u_0) = -2^7/3^5 \approx -0.526749$ and $f(u_0) = 2^{12}/3^9 \approx 0.208098$.

Figure 4 shows the dependence of the scaled energy ε_e on the scaled electric field f. It is seen that there exists a critical value f_c such that for each $f < f_c$ there are two equilibrium (classical) states of different energies. At $f = f_c$ the energies of the two equilibrium states become equal to each other, while for $f > f_c$ there is no dynamic equilibrium at all. It turns out that critical value f_c and the critical energy ε_{ec} (where the two branches in Fig. 4 undergo a V-shape crossing) corresponds to the extrema $f(u_0)$ and $\varepsilon_e(u_0)$, respectively:

$$f_c = 2^{12}/3^9 \approx 0.208098, \quad \varepsilon_{ec} = -2^7/3^5 \approx -0.526749. \quad (21)$$

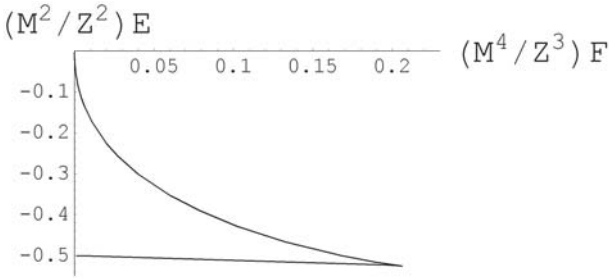

Fig. 4. Dependence of the scaled energy EM^2/Z^2 on the scaled electric field FM^4/Z^3 at the absence of the magnetic field.

Physically, as the electric field starts increasing from zero, the plane of the classical orbit shifts (see Eq. (18)) and the radius of the orbit starts increasing (see Fig. 3). However, for each $f < f_c$ there are two values of the scaled equilibrium radius of the orbit (see Fig. 3) — we denote them u_1 and $u_2 > u_1$. A simple analysis shows that u_1 and the lower energy branch in Figure 4 correspond to the stable equilibrium, while u_2 and the upper energy branch in Figure 4 correspond to the unstable equilibrium[2]. In other words, the critical scaled field f_c from equation (21) is the classical ionization threshold.

We note that the critical scaled field f_c for CRS from equation (21) is by a factor of 3.3 greater than the standard result for "general" Rydberg states $f_{c,G} = 1/16 \approx 0.0625$ (see, e.g., [16]). Physically this is because the ionization from circular orbits is more difficult to achieve than from non-circular orbits.

It is also instructive to compare our classical results for f_c and ε_{ec} with the corresponding quantal results by Kolosov [17] (based on the previous papers by Damburg and Kolosov [18–20]) derived in the parabolic quantization $\{n_1,\ n_2,\ m\}$. For CRS, i.e. for parabolic quantum numbers $\{0, 0, n-1\}$, his results are as follows:

$$f_{c,K} = 2^{1/2}/\left[3\pi(0.92)^3\right] \approx 0.193,$$
$$\varepsilon_{ec,K} = -1/\left[2(0.92)^2\right] \approx -0.591. \qquad (22)$$

Thus, Kolosov overestimated ε_{ec} by over 12% and underestimated f_c by over 7%. This is because his results were valid only for a relatively small electric field F and represented the first term of an expansion in terms of a small parameter $F/(-2E)^{3/2}$.

We note that authors of the previous studies of classical CRS in an electric field [9,10] already obtained the dependence of ε_e on f in a one-parametric form (though in different parameterizations) and derived the critical values f_c and ε_{ec}. We presented similar results for two reasons. First, while studying classical CRS in collinear electric and magnetic fields (which is the main focus of the present work), it is convenient to have in the same paper — for the comparison — the results for the two important particular cases: classical CRS in a magnetic field only and classical CRS in an electric field only. Second, we complemented our analytical results, which are similar to those from [9,10], by the universal plot of the scaled energy ε_e versus the scaled electric field f (Fig. 4), as well as by the universal plots $\varepsilon_e(u)$ and $f(u)$ showing the dependence of these physical quantities on the scaled equilibrium radius of the orbit (Fig. 3). In our view, Figures 3 and 4 reveal some important details helping to better understand the physics behind the studied phenomenon. Besides, due to the employment of the scaled quantities, both Figure 3 and Figure 4 present the results for all possible sets of M, Z, and B in one or two universal curves.

5 Classical circular Rydberg states in collinear electric and magnetic fields of arbitrary strengths

Now we analyze the general form of the scaled Hamiltonian given by equation (3). The conditions of the dynamic equilibrium are:

$$\partial h/\partial u = -1/u^3 + u/\left(u^2+w^2\right)^{3/2} + \omega^2 u = 0, \qquad (23)$$
$$\partial h/\partial w = w/\left(u^2+w^2\right)^{3/2} + f = 0. \qquad (24)$$

From equation (23) we find the following relation between the equilibrium values of w and u at any given value of the scaled magnetic field ω:

$$w(u,\omega) = -u\left\{\left[u/\left(1-\omega^2u^4\right)\right]^{2/3} - 1\right\}^{1/2}. \qquad (25)$$

Using equations (24, 25), we express the scaled electric field f via the scaled radius of the orbit u at any given value of the scaled magnetic field ω:

$$f(u,\omega) = (1/u^4-\omega^2)^{2/3}\left[1-u^2\left(1/u^4-\omega^2\right)^{2/3}\right]^{1/2}. \qquad (26)$$

Substituting $w(u)$ and $f(u)$ from equations (25, 26) into equation (3), we obtain the following result for the dependence of the scaled energy ε on the scaled radius of the orbit u at any given value of the scaled magnetic field ω:

$$\varepsilon(u,\omega) = 3/\left(2u^2\right) + \omega - \omega^2u^2/2 - 2\left(1/u^4-\omega^2\right)^{1/3}. \qquad (27)$$

At any given value of the scaled magnetic field ω, equations (26, 27) represent the dependence of the scaled energy ε on the scaled electric field f in the one-parametric form $\{\varepsilon(u), f(u)\}$. The allowed range of the scaled radius of the orbit u is controlled by the scaled magnetic field ω:

$$g\left(|\omega|^{2/3}\right)/|\omega|^{2/3} \le u \le 1/|\omega|^{1/2}, \qquad (28)$$

where $g(x)$ is defined by equation (11).

Figure 5 shows the dependence of the scaled shift w of the orbital plane versus the scaled radius of the orbit u for

[2] The situation is similar to the results presented in Appendix and to other results we obtained in [14,15] for the classical problem of two Coulomb centers. In the studies [14,15] we also found that out of the two crossing energy branches, only the lower branch corresponded to the stable equilibrium, while the upper branch corresponded to the unstable equilibrium.

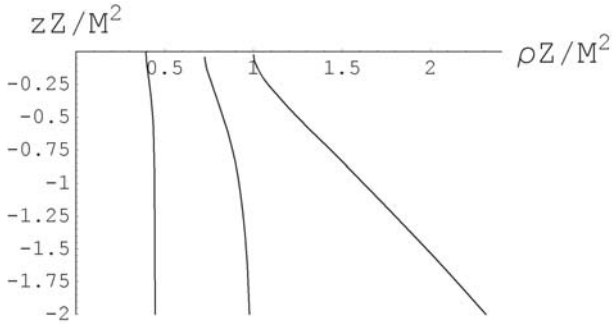

Fig. 5. Dependence of the scaled shift zZ/M^2 of the orbital plane versus the scaled radius of the orbit $\rho Z/M^2$ for three different absolute values of the scaled magnetic field $\omega \equiv \Omega M^3/Z^2$: $\omega = 0$ (the right curve), $|\omega| = 1$ (the middle curve), and $|\omega| = 5$ (the left curve).

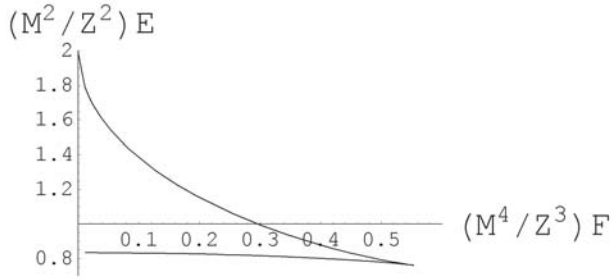

Fig. 6. Dependence of the scaled energy $\varepsilon \equiv EM^2/Z^2$ on the scaled electric field $f \equiv FM^4/Z^3$ at the scaled magnetic field $\omega = 1$.

three different absolute values of the scaled magnetic field: $\omega = 0$ (the right curve), $|\omega| = 1$ (the middle curve), and $|\omega| = 5$ (the left curve). It is seen that as $|\omega|$ increases, the dependence $w(u)$ becomes steeper. Physically this is due to the following. The magnetic field decreases the radius of the orbit, but does not shift the orbital plane. The electric field increases the radius of the orbit and shifts the orbital plane. Therefore, for a given radius of the orbit ρ_0, as the magnetic field increases, it takes a larger electric field to maintain $\rho = \rho_0$. The increased electric field causes a larger shift of the orbital plane at the same $\rho = \rho_0$.

Figures 6 and 7 show the dependence of the scaled energy ε on the scaled electric field f for $\omega = 1$ and $\omega = -1$, respectively. The extrema of the functions $\varepsilon(u, \pm 1)$ and $f(u, \pm 1)$ in equations (26, 27) correspond to the V-shape crossing of the two energy branches in Figures 6 and 7. From the comparison with Figures 3 and 4 it is seen that the magnetic field increased the value of the critical field f_c, corresponding to the classical ionization threshold.

Figures 8 and 9 show the dependence of the scaled energy ε on the scaled electric field f for $\omega = 10$ and $\omega = -10$, respectively. The extrema of the functions $\varepsilon(u, \pm 10)$ and $f(u, \pm 10)$ in equations (26, 27) correspond to the V-shape crossing of the two energy branches in Figures 8 and 9. From the comparison with Figures 6, 7 it is seen that the relatively large magnetic field further

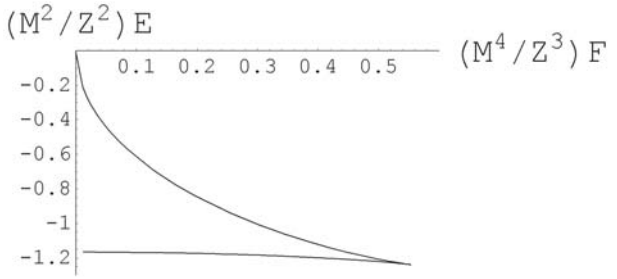

Fig. 7. Dependence of the scaled energy $\varepsilon \equiv EM^2/Z^2$ on the scaled electric field $f \equiv FM^4/Z^3$ at the scaled magnetic field $\omega = -1$.

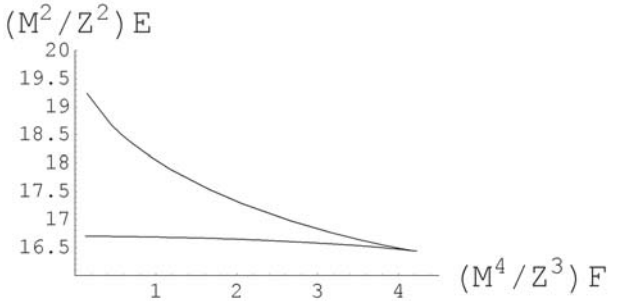

Fig. 8. Dependence of the scaled energy $\varepsilon \equiv EM^2/Z^2$ on the scaled electric field $f \equiv FM^4/Z^3$ at the scaled magnetic field $\omega = 10$.

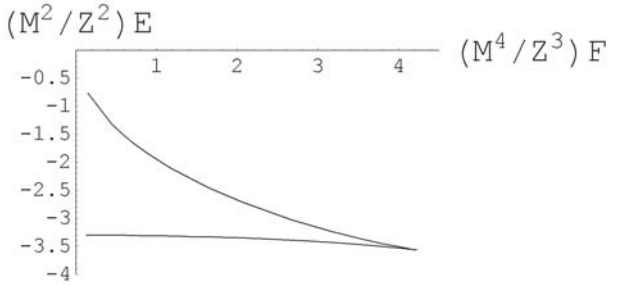

Fig. 9. Dependence of the scaled energy $\varepsilon \equiv EM^2/Z^2$ on the scaled electric field $f \equiv FM^4/Z^3$ at the scaled magnetic field $\omega = -10$.

increased the value of the critical field f_c, corresponding to the classical ionization threshold.

In Figures 6–9, the energy curve in the region $\omega > 0$, corresponding to parallel electric and magnetic fields, differs from the energy curve in the region $\omega < 0$, corresponding to antiparallel electric and magnetic fields. The difference is due to the second (paramagnetic) term in equation (27). In distinction, the scaled electric field given by equation (26) is symmetric with respect to the change of the sign of ω.

Physically, the results of this section combined with the results presented in Sections 3 and 4 demonstrate the following. As noted above, the electric field increases the radius of the orbit and shifts the plane of the orbit. Thus, it works as a destabilizing factor: as the electric field reaches some critical value f_c, the motion becomes unstable and the system gets ionized. The magnetic field decreases the

radius of the orbit. Thus it works as a stabilizing factor: the greater the magnetic field, the greater the electric field is required for reaching the classical ionization threshold. A detailed study of the stability is presented in Appendix.

It would be instructive to compare our classical results with the corresponding quantal results for CRS. However, for the case of parallel electric and magnetic fields, while some quantal results for the energy are available for $|m| \ll n$ (see, e.g., [20,21]), there are no explicit results for the energy of CRS (i.e., for $|m| = n - 1 \gg 1$) — to the best of our knowledge. From [20,21] it is known that for $|m| > n/5^{1/2} \gg 1$, the quantal energy $\varepsilon_q(f,\omega)$ in the parallel fields should have the following general structure

$$\varepsilon_Q(f,\omega) = \sum_{p,r=0}^{\infty} a_{pr} f^p \omega^r, \tag{29}$$

where $a_{pr} = 0$ if p or r is odd, except a_{01}. If we disregard terms where $p + r \geq 4$, then the effects of the parallel electric and magnetic fields would simply superpose (as first mentioned by Bethe [23]). Therefore, in this case we can complement the "magnetic" quantal result from equation (14) by the well-known expression for the quadratic Stark effect (see, e.g., [24]). In this way, for $|m| = n-1 \gg 1$ we obtain the following quantal result

$$\begin{aligned}\varepsilon_Q(f,\omega) \approx -1/2 - [1 + 9/(4n)]f^2/2 \\ + \omega + [1 \pm 2(2N_\pm + 1)/n]\omega^2/2; \\ N_\pm = 0, 1, 2, \ldots;\ N_\pm \ll n.\end{aligned} \tag{30}$$

On the one hand, the quantal result includes small corrections $\sim 1/n$ (the second term in each of the brackets in Eq. (30)), which would not follow from our classical result (26, 27). On the other hand, the quantal result is valid only for small values of both the scaled electric field $|f| \ll 1$ and the scaled magnetic field $|\omega| \ll 1$, while our classical result is valid for arbitrary values of both fields, including the strong field regions.

The quantal small-field result from equation (30) can be derived from our classical formulas (26, 27) in the following approximation. First, we seek the scaled radius of the orbit u in the form: $u = 1 + q(f,\omega)$, where $q(f,\omega) \ll 1$. Second, we substitute $u = 1 + q(f,\omega)$ in equations (26, 27) and expand their right sides in terms of q and ω^2 up to the first order with respect to either q or ω^2. In this way, from equation (26) we obtain: $q(f,\omega) \approx 3f^2 - \omega^2$. By substituting this approximate result for $q(f,\omega)$ into (already expanded) equation (27), we retrieve the quantal small-field result from equation (30), apart from the small corrections $\sim 1/n$.

To give a sentiment of the inaccuracy of the quantal result (30), caused by the disregard of the higher order terms with respect to f and ω, we use as an example a set of $\{f = 1/3, \omega = 1/2\}$. From equation (30) for $n \gg N_\pm$ we find $\varepsilon_Q(1/3, 1/2) = 5/72 \approx 0.0695$, while our corresponding classical result is $\varepsilon(1/3, 1/2) \approx 0.0620$. Thus, already at these relatively small values of f and ω, the quantal result has an error of about 12%. Obviously, the inaccuracy of the quantal result would increase with the growth of f or ω.

Let us now study the classical ionization threshold in more detail: how the critical value of the scaled electric field f_c and the corresponding critical values of the scaled energy ε_c and of the scaled radius of the orbit u_c depend on the scaled magnetic field ω. First, from the equation $\partial\varepsilon(u,\omega)/\partial u = 0$ we find $u_c(\omega)$. Then we substitute $u_c(\omega)$ into equations (26, 27) and find $f_c(\omega)$ and $\varepsilon_c(\omega)$. As a result, we find the following.

For the critical value of the scaled radius of the orbit:

$$\begin{aligned} u_c &\approx (9/8)^{3/2}\left(1 + 3^{12}\,\omega^2/2^{19}\right), && |\omega| \ll 1; \\ u_c &\approx 0.81622, && |\omega| = 1; \\ u_c &\approx \left(1/|\omega|^{1/2}\right)\left[1 - 1/(54|\omega|)^{1/2}\right], && |\omega| \gg 1. \end{aligned} \tag{31}$$

For the critical value of the scaled electric field:

$$\begin{aligned} f_c &\approx 2^{12}/3^9 + 27\omega^2/32, && |\omega| \ll 1; \\ f_c &\approx 0.55214, && |\omega| = 1; \\ f_c &\approx 2|\omega|/3^{3/2} + 2^{3/2}|\omega|^{1/2}/27, && |\omega| \gg 1. \end{aligned} \tag{32}$$

For the critical value of the scaled energy:

$$\begin{aligned} \varepsilon_c &\approx -2^7/3^5 + \omega + 3^6\omega^2/2^{11}, && |\omega| \ll 1; \\ \varepsilon_c &\approx 0.76223, && |\omega| = 1; \\ \varepsilon_c &\approx 2\omega - 2^{5/2}|\omega|^{1/2}/3^{3/2}, && \omega \gg 1; \\ \varepsilon_c &\approx 2^{5/2}|\omega|^{1/2}/3^{3/2}, && \omega \ll -1. \end{aligned} \tag{33}$$

Based on equations (32, 33), we developed the following closed-form expressions for f_c and ε_c valid for arbitrary ω:

$$f_c = 2^{12}/3^9 + 54\omega^2/[64 - 27(2|\omega|)^{1/2} + 3^{1/2}81|\omega|]; \tag{34}$$

$$\begin{aligned}\varepsilon_c \approx -2^7/3^5 + \omega + \omega^2/(1 + |\omega|) \\ - (2^{5/2}/3^{3/2})\omega^2/(4.1902 + |\omega|^{3/2}).\end{aligned} \tag{35}$$

These closed-form expressions for f_c and ε_c reproduce exactly the first two terms of the corresponding expansions at both $|\omega| \ll 1$ and $|\omega| \gg 1$; for any ω they have a relative inaccuracy of about 3% or less.

Figure 10 shows the dependencies of the $\varepsilon_c(\omega)$ and $f_c(\omega)$. With respect to the change of the sign of ω, the function $f_c(\omega)$ is symmetric, while the function $\varepsilon_c(\omega)$ is asymmetric — due to the second (paramagnetic) term in equation (35).

We note that the authors of [8] gave explicit expressions for the energy E only for the region of a weak electric field F and only in the limits of $B \to 0$ and $B \to \infty$. As for the values of the electric field F_c and of the energy E_c at the classical ionization threshold, paper [8] presented $F_c(B)$ only for the limits $B \to 0$ and $B \to \infty$ and did not present $E_c(B)$ at all.

6 Conclusions

We derived analytical expressions for the energy E of classical CRS of hydrogenlike systems in collinear electric (**F**)

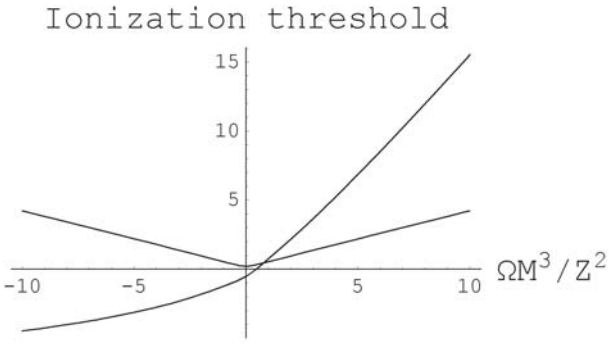

Fig. 10. Dependence of the critical value of the scaled electric field $f_c \equiv F_c M^4/Z^3$ at the classical ionization threshold (symmetric curve) and of the critical value of the scaled energy $\varepsilon_c \equiv E_c M^2/Z^2$ at the classical ionization threshold (asymmetric curve) on the scaled magnetic field $\omega \equiv \Omega M^3/Z^2$.

and magnetic (**B**) fields of arbitrary strengths. Previously published explicit expressions for the energy E were given only for the region of a weak electric field F and only in the limits of $B \to 0$ and $B \to \infty$ [8].

We offered formulas for the dependence of the classical ionization threshold $F_c(B)$ and of the energy at this threshold $E_c(B)$ valid for the magnetic field B of an arbitrary strength. Previously published paper [8] presented $F_c(B)$ only for the limits $B \to 0$ and $B \to \infty$ and did not present $E_c(B)$ at all.

In addition, for two important particular cases previously studied in the literature — classical CRS in a magnetic field only [9] and classical CRS in an electric field only [10] — we presented some new results as well. For classical CRS in a magnetic field of an arbitrary strength we obtained a direct (non-parametric) analytical solution $E(B)$. In distinction, in [9], the dependence of the energy E on the magnetic field B was presented, in fact, only in a one-parametric form: $\{E(u), B(u)\}$. For classical CRS in an electric field of an arbitrary strength we complemented the results from [10] by a universal plot of a scaled energy versus a scaled electric field, thus presenting all possible subcases for this problem in one curve.

We believe the fundamental importance of our analytical results is due to the fact that hydrogenlike systems in external fields were and remain a test-bed for atomic physics. We also believe that our results (e.g., the new ionization threshold (34)) would have a practical importance as well: we hope they would motivate experiments on a *magnetic control of the ionization instability of CRS*. They should be especially relevant to such new, rapidly developing area of experimental research as cold Rydberg plasmas [25–27]. Indeed, in plasmas, including cold Rydberg plasmas, the intrinsic electric microfield causes a phenomenon of "continuum lowering" (see, e.g. [28–30] and references therein), which significantly affects radiative properties of these media. Our results could be used as a theoretical basis for setting up experiments on a *magnetic control of the continuum lowering in cold Rydberg plasmas*. Another area of the potential importance of our results is the production of Rydberg states of anti-hydrogen in strong electric and magnetic fields [31], where the field-caused ionization is the primary concern.

Appendix: Going beyond the circular states

In this appendix we relax the assumption of circular orbits of the electron: we consider the dynamics of the oscillatory motion around equilibrium circular orbits. This general case still allows an important simplification (due to the conservation of the z-component of the angular momentum): the z- and ρ-motions can be determined separately from the φ-motion. Then the φ-motion can be found from the ρ-motion as shown below.

In the scaled variables from equation (2), the z- and ρ-motions correspond to w- and u-motions, respectively. The scaled Hamiltonian $h(u, w)$ for CRS, given by equation (3), plays the role of the Scaled Potential Energy (SPE) for the general type of the motion considered in this appendix. To emphasize this point, we use below the notation $v(u, w)$ for the SPE, even though the explicit expression for $v(u, w)$ is the same as for $h(u, w)$:

$$v(u,w) = 1/(2u^2) - 1/(u^2+w^2)^{1/2} + fw + \omega + \omega^2 u^2/2. \tag{A.1}$$

The equilibrium points (w_0, u_0) of the SPE can be found from the equations $\partial v/\partial u = \partial h/\partial u = 0$ (compare to Eqs. (23, 24)). They are interrelated as follows:

$$w_0(u_0) = -u_0 \left\{ \left[u_0/\left(1 - \omega^2 u_0^4\right)\right]^{2/3} - 1 \right\}^{1/2} \tag{A.2}$$

(compare to Eq. (25)). We assign the subscript "zero" to the equilibrium values of w and v to emphasize the distinction of the general case considered in this appendix from CRS analyzed in Section 5. Equation (A.2) determines a line $w_0(u_0)$ in the plane (w, v), where the equilibrium points are located.

Now we expand the SPE $v(u, w)$ in terms of δw and δv, where

$$\delta w \equiv w - w_0, \quad \delta u \equiv u - u_0. \tag{A.3}$$

The expansion has the form:

$$v \cong v_0 + v_{ww}(\delta w)^2/2 + v_{uu}(\delta u)^2/2 + v_{wu}(\delta w)(\delta u),$$
$$v_0 \equiv v(w_0, u_0). \tag{A.4}$$

The second derivatives of the SPE in equation (A.4) are

$$v_{ww} \equiv (\partial^2 v/\partial w^2)_0 = (u_0^2 - 2w_0^2)/(w_0^2 + u_0^2)^{5/2},$$
$$v_{uu} \equiv (\partial^2 v/\partial u^2)_0 = 3/u_0^4 + \omega^2 + (w_0^2 - 2u_0^2)/(w_0^2 + u_0^2)^{5/2},$$
$$v_{wu} \equiv (\partial^2 v/\partial w \partial u)_0 = -3w_0 u_0/(w_0^2 + u_0^2)^{5/2}. \tag{A.5}$$

Here the suffix 0 at the derivatives means that after the differentiation one should set $u = u_0$ and $w = w_0(u_0)$, where $w_0(u_0)$ is given by equation (A.2).

Since generally $v_{wu} \leq 0$, a rotation of the reference frame is required in order to transform the SPE to so-called "normal" coordinates, diagonalizing the matrix of the second derivatives of the SPE [32,33]:

$$\delta w' = \delta w \cos\alpha + \delta u \sin\alpha, \quad \delta u' = -\delta w \sin\alpha + \delta u \cos\alpha. \tag{A.6}$$

It is easy to find that

$$\begin{aligned}\tan 2\alpha &= 2v_{wu}/(v_{ww} - v_{uu}) \\ &= 2w_0u_0/[w_0^2 - u_0^2 + (1/u_0^4 + \omega^2/3)(w_0^2 + u_0^2)^{5/2}].\end{aligned} \tag{A.7}$$

Then $\cos\alpha$ and $\sin\alpha$ can be expressed via $\tan 2\alpha$ from equation (A.7) by well-known formulas:

$$\begin{aligned}\cos\alpha &= \Big\{[1 - (1 + \tan^2 2\alpha)^{-1/2}]/2\Big\}^{1/2}, \\ \sin\alpha &= \Big\{[1 + (1 + \tan^2 2\alpha)^{-1/2}]/2\Big\}^{1/2} \mathrm{sign}(\tan 2\alpha).\end{aligned} \tag{A.8}$$

In the normal coordinates, the SPE takes the form

$$v \cong v_0 + \delta w'^2\, \omega_-^2/2 + \delta u'^2\, \omega_+^2/2, \tag{A.9}$$

where

$$\begin{aligned}\omega_\pm(u_0,\omega) \equiv 2^{-1/2}\Big\{ & g_1(u_0,\omega) \pm [g_1^2(u_0,\omega) \\ & + 4g_2(u_0,\omega)]^{1/2} \mathrm{sign}[g_0(u_0,\omega)]\Big\}^{1/2}.\end{aligned} \tag{A.10}$$

Here

$$\begin{aligned}g_0(u_0,\omega) &\equiv v_{ww} - v_{uu} = -3[1/u_0^4 + \omega^2/3 \\ &\quad + (w_0^2 - u_0^2)/(w_0^2 + u_0^2)^{5/2}], \\ g_1(u_0,\omega) &\equiv v_{ww} + v_{uu} = 3/u_0^4 + \omega^2 - 1/(w_0^2 + u_0^2)^{3/2}, \\ g_2(u_0,\omega) &\equiv v_{wu}^2 - v_{ww}v_{uu} = 2/(w_0^2 + u_0^2)^3 \\ &\quad - (3/u_0^4 + \omega^2)(u_0^2 - 2w_0^2)/(w_0^2 + u_0^2)^{5/2}.\end{aligned} \tag{A.11}$$

We remind again that w_0 in above formulas stands for the function $w_0(u_0)$ given by equation (A.2).

From equation (A.10) it is seen that both the scaled frequencies ω_+ and ω_- are real if

$$g_2(u_0,\omega) < 0. \tag{A.12}$$

(We note that the corresponding dimensional frequencies $\Omega_\pm$ are related to $\omega_\pm$ as follows: $\omega_\pm = \Omega_\pm M^3/Z^2$ — compare to Eq. (2).) Thus, under the condition (A.12), the SPE has a two-dimensional minimum at the equilibrium values of u_0 and $w_0(u_0)$, so that the equilibrium is stable. Physically, in this case ω_+ and ω_- are scaled frequencies of small oscillations around the equilibrium in the directions of the normal coordinates $\delta u'$ and $\delta w'$, respectively. This situation corresponds to the lower branch of the scaled energy in Figures 6–9.

Introducing a scaled (dimensionless) time

$$\tau \equiv tZ^2/M^3, \tag{A.13}$$

we obtain the final expression for the small oscillations around the stable equilibrium in the form:

$$\begin{aligned}\delta w(\tau) &= a_w[\cos(\omega_-\,\tau + \psi_w)]\cos\alpha \\ &\quad - a_u \cos(\omega_+\,\tau + \psi_u]\sin\alpha, \\ \delta u(\tau) &= a_w[\cos(\omega_-\,\tau + \psi_w)]\sin\alpha \\ &\quad + a_u \cos(\omega_+\,\tau + \psi_u]\cos\alpha.\end{aligned} \tag{A.14}$$

Here amplitudes a_w, a_u and phases ψ_w, ψ_u are determined by initial conditions; sinα and cosα are given by equations (A.7, A.8).

The equation for the φ-motion can be written in the scaled notations as

$$d\varphi/d\tau = 1/u^2. \tag{A.15}$$

Substituting in equation (A.15) $u(\tau) \cong u_0 + \delta u(\tau)$, where $\delta u(\tau)$ is given by equation (A.14) and integrating over τ, we obtain the solution for the φ-motion

$$\begin{aligned}\varphi(\tau) \cong \tau/u_0^2 - 2\Big\{ & \omega_-^{-1} a_w[\sin(\omega_-\tau + \psi_w) - \sin\psi_w]\sin\alpha \\ & + \omega_+^{-1} a_u[\sin(\omega_+\tau + \psi_u) - \sin\psi_u)]\cos\alpha\Big\}/u_0^3.\end{aligned} \tag{A.16}$$

Equation (A.16) shows that the φ-motion is a rotation about the axis of symmetry (defined by the direction of the parallel fields) with the scaled frequency $1/u_0^2$, slightly modulated by oscillations of the scaled radius of the orbit u at the frequencies ω_+ and ω_-. In other words, the motion of the electron occurs on a conical surface of the averaged radius u_0.

If $g_2(u_0,\omega) > 0$, the equilibrium is unstable: either ω_+ or ω_- takes imaginary values. If, say ω_- is imaginary, its absolute value $|\omega_-|$ is the increment of the instability developing in the direction of the normal coordinate $\delta w'$. This situation corresponds to the upper branch of the scaled energy in Figures 6–9.

If $g_2(u_0,\omega) = 0$, then ω_+ and ω_- are real and equal to each other. This situation corresponds to the V-shape crossing of the upper and lower branches of the scaled energy in Figures 6–9, that is to the classical ionization threshold.

Finally we emphasize that equation (A.10) for $\omega_\pm(u_0,\omega)$ together with equation (26) for $f(u_0,\omega)$ represent the analytical dependence of $\omega_\pm$ on the scaled magnetic field ω and on the scaled electric field f in a one-parametric form (via u_0) for arbitrary strengths of both fields. We note that the authors of [8] gave explicit expressions for $\omega_\pm$ only for the small field region.

References

1. E. Lee, D. Farrelly, T. Uzer, Opt. Expr. **1**, 221 (1997)
2. T.C. Germann, D.R. Herschbach, M. Dunn, D.K. Watson, Phys. Rev. Lett. **74**, 658 (1995)

3. C.H. Cheng, C.Y. Lee, T.F. Gallagher, Phys. Rev. Lett. **73**, 3078 (1994)
4. L. Chen, M. Cheret, F. Roussel, G. Spiess, J. Phys. B **26**, L437 (1993)
5. S.K. Dutta, D. Feldbaum, A. Walz-Flannigan, J.R. Guest, G. Raithel, Phys. Rev. Lett. **86**, 3993 (2001)
6. R.G. Hulet, E.S. Hilfer, D. Kleppner, Phys. Rev. Lett. **55**, 2137 (1985)
7. K.B. MacAdam, E. Horsdal-Petersen, J. Phys. B **36**, R167 (2003)
8. V.M. Vainberg, V.S. Popov, A.V. Sergeev, Sov. Phys. JETP **71**, 470 (1990)
9. C.M. Bender, L.D. Mlodinow, N. Papanicolaou, Phys. Rev. A **25**, 1305 (1982)
10. V.M. Vainberg, V.D. Mur, V.S. Popov, A.V. Sergeev, Sov. Phys. JETP **66**, 258 (1987)
11. H. Ruder, G. Wunner, H. Herold, F. Geyer, *Atoms in Strong Magnetic Fields* (Springer, Berlin, 1994)
12. V.S. Lisitsa, *Atoms in Plasmas* (Springer, Berlin, 1994)
13. P.A. Braun, Sov. Phys. JETP **57**, 492 (1983)
14. E. Oks, Phys. Rev. Lett. **85**, 2084 (2000)
15. E. Oks, J. Phys. B: Atom. Mol. Opt. Phys. **33**, 3319 (2000)
16. T.F. Gallagher, *Rydberg Atoms* (Cambridge, Cambridge University Press, 1994).
17. V.V. Kolosov, J. Phys. B **16**, 25 (1983)
18. R.J. Damburg, V.V. Kolosov, J. Phys. B **12**, 2637 (1979)
19. R.J. Damburg, V.V. Kolosov, J. Phys. B **11**, 1921 (1978)
20. R.J. Damburg, V.V. Kolosov, J. Phys. B **9**, 3149 (1976)
21. A.P. Kazantsev, V.L. Pokrovsky, JETP Lett. **37**, 557 (1983)
22. A.P. Kazantsev, V.L. Pokrovsky, J. Bergou, Phys. Rev. A **28**, 3659 (1983)
23. H.A. Bethe, *Quantenmechanik der Ein- und Zwei-Elektronenprobleme*, Handbuch der Physik (Springer, Berlin, 1933), Bd. **24**/1
24. L.D. Landau, E.M. Lifshitz, *Quantum Mechanics* (Pergamon, Oxford, 1965)
25. T.C. Killian, M.J. Lim, S. Kulin, R. Dumke, S.D. Bergeson, S.L. Rolston, Phys. Rev. Lett. **86**, 3759 (2001)
26. T.C. Killian, S. Kulin, S.D. Bergeson, L.A. Orozco, C. Orzel, S.L. Rolston, Phys. Rev. Lett. **83**, 4776 (1999)
27. M.P. Robinson, B.L. Tolra, M.W. Noel, T.F. Galagher, P. Pillet, Phys. Rev. Lett. **85**, 4466 (2000)
28. E. Oks, Phys. Rev. E **63**, 057401 (2001)
29. D. Salzmann, *Atomic Physics in Hot Plasmas* (Oxford Univ. Press, Oxford, 1998), Chaps. 2, 3
30. H.R. Griem, *Principles of Plasma Spectroscopy* (Cambridge Univ. Press, Cambridge, 1997), Sects. 5.5, 7.3
31. M. Amoretti, C. Amsler, G. Bonomi, A. Bouchta, P. Bowe, C. Carraro, C.L. Cesar, M. Charlton, M.J.T. Collier, M. Doser, V. Filippini, K.S. Fine, A. Fontana, M.C. Fujiwara, R. Funakoshi, P. Genova, J.S. Hangst, R.S. Hayano, M.H. Holzscheiter, L.V. Jorgensen, V. Lagomarsino, R. Landua, D. Lindelöf, E.L. Rizzini, M. Macri, N. Madsen, G. Manuzio, M. Marchesotti, P. Montagna, H. Pruys, C. Regenfus, P. Riedler, J. Rochet, A. Rotondi, G. Rouleau, G. Testera, A. Variola, T.L. Watson, D.P. van der Werf, Nature **419**, 456 (2002)
32. L.D. Landau, E.M. Lifshitz, *Mechanics* (Pergamon, Oxford, 1960)
33. H. Goldstein, *Classical Mechanics* (Addison-Wesley, Reading MA, 1980)